John M. Haschke

Contribution from the Department of Chemistry,
University of Michigan, Ann Arbor, Michigan 48104

Preparation, Phase Equilibria, and Crystal Chemistry of Samarium Bromides

JOHN M. HASCHKE

Received April 16, 1975 AIC50265G

The preparative reactions, phase equilibria, and some properties of the anhydrous samarium bromides have been investigated. The use of hydrogen and metallic reduction procedures have resulted in the identification of two phases near the dibromide composition. At all temperatures up to 750°C, red $PbCl_2$-type and black $SrBr_2$-type phases coexist only with samarium metal and with the higher bromide ($SmBr_{2.129}$), respectively. Intermediate bromides ($SmBr_{2.129(8)}$, $SmBr_{2.140(10)}$, and $SmBr_{2.172(8)}$) which correspond closely with the compositions Sm_6Br_{13}, Sm_7Br_{15}, and Sm_8Br_{17}, respectively, have also been identified. The formation of hydrated phases ($SmBr_2 \cdot H_2O$ and $SmBr_3 \cdot 6H_2O$) has been observed and x-ray diffraction data for the bromides and hydrated bromides are reported. The observed intermediate bromides and numerous intermediate lanthanide halides reported in the literature have been described by the homologous series M_nX_{2n+1}. The phase equilibria, crystal chemistry, and possible structural origins of the homologous series phases are discussed.

Introduction

The preparation and certain properties of samarium dibromide were described by workers in Germany approximately 45 years ago,[1,2] but structural data have not been reported. A subsequent x-ray study of metal dihalides[3] showed that the dibromides of strontium, samarium, and europium are isostructural. The structure of strontium dibromide[4] and the structural and thermodynamic properties of europium dibromide[5,6] have only recently been described.

In an effort to complete the structural characterization of this group of dibromides, an examination of the samarium phase was initiated. After preliminary results indicated the existence of an intermediate composition between those of the dibromide and the tribromide, a thorough investigation of the samarium–bromine system was pursued.

Experimental Section

Samarium dibromide was prepared by reduction of the tribromide. Samples of $SmBr_3$ were obtained from Sm_2O_3 (99.9%, American Potash and Chemical Co.) by the ammonium halide matrix method described previously[6] and were reduced both with hydrogen (prepurified, Matheson) and with samarium metal (99.9% ingot, Research Chemicals). The tribromide (2–3 g) was placed in a degassed graphite boat and transferred to a liquid nitrogen trapped Vycor vacuum system (residual pressure $< 5 \times 10^{-6}$ Torr) which was flushed and back-filled with H_2. Flow conditions (H_2 at 1 atm and 10–20 cm^3/min) and static atmospheres (0.8 atm of H_2) were employed during thermal cycles in which the samples were heated at 900°C by an external resistance furnace for 2–5 hr and cooled rapidly (10 min) to room temperature. Mixtures (0.2–0.5 g) of $SmBr_3$ and Sm chips were prepared and placed in tubes (6.3-mm i.d. × 40-mm length) of SiO_2, C, Ta, or Au, sealed in evacuated quartz ampules, heated at 700–800°C for periods up to 5 hr, and cooled rapidly. Tantalum and gold containers were crimped shut to restrict the loss of samarium vapor. Since all of the container materials are potential samarium scavengers, slight stoichiometric excesses of metal were routinely added.

Phase equilibria of the dibromide were investigated by thermal quenching experiments and by the reaction of dibromide with samarium metal and with tribromide. The possible existence of a thermally induced transition was examined with samples (0.2–0.3 g) of $SmBr_2$ which were placed in Au capsules, sealed in evacuated quartz ampules, heated for several hours at selected temperatures in the range 500–900°C, and quenched by direct immersion in water. In an effort to check for the existence of lower bromide compositions and to determine if the dibromide exhibited variations in composition, mixtures of $SmBr_2$ and Sm were allowed to react. Samples with Br:Sm ratios, x, between 1.75 and 2.00 were placed in graphite boats and heated rapidly to 700–750°C under vacuum. The loss of metal vapor was minimized by short heating cycles (0.5–1 hr) and rapid cooling of the products.

Equilibria in the composition range $2.0 < x < 3.0$ were investigated by the reaction of dibromide–tribromide mixtures which were prepared according to eq 1. Quantities (0.2–0.5 g) of selected compositions were mixed thoroughly, sealed in gold-lined quartz ampules, and allowed to react for 1 hr at 700–800°C. Products were cooled to room temperature by three different procedures: water quenching, rapid cooling (10 min), and annealing at 450° for 15 hr. Large samples (1–2 g) of the mixtures were placed in graphite boats with tightly fitting Au foil covers, heated rapidly to 800°C under vacuum, and annealed at 450° for 5 hr before cooling. Because of material loss during heating under dynamic vacuum, several additions of tribromide were generally required for attainment of the desired product.

$$SmBr_2 + [(x-2)/(3-x)]SmBr_3 \rightarrow [1/(3-x)]SmBr_x \quad (1)$$

Table I. Analytical Results for Crystallographically Pure Samples of Samarium Bromide Phases

Phase	% Sm	%Br	Br:Sm	% Sm	% Br	Br:Sm
$SmBr_2$	48.48 (10)	51.46 (13)	1.997 (9)	48.47	51.53	2.000
Sm_8Br_{17}	46.95 (9)	53.14 (11)	2.129 (8)	46.96	53.04	2.125
Sm_7Br_{15}	46.72 (10)	53.15 (13)	2.140 (10)	46.75	53.25	2.143
Sm_6Br_{13}	46.41 (7)	53.58 (11)	2.172 (8)	46.48	53.52	2.167
$SmBr_3$	38.50 (9)	61.52 (10)	3.004 (9)	38.54	61.46	3.000

[a] The uncertainty in the last digit appears in parentheses. [b] All results except that of $SmBr_3$ have been corrected for SmOBr contamination. (In the absence of corrections, the sums of Br and Sm contents account for approximately 99.5% of the sample masses, and the apparent Br/Sm ratios are lower than the corrected values by 0.03–0.05.)

Reaction products were analyzed by chemical and x-ray diffraction methods. Powder x-ray diffraction data were obtained with an evacuated 114.6-mm diameter Guinier-Haegg camera using Cu $K\alpha_1$ radiation and silicon (a_0 = 5.43062 Å) as an internal standard; Weissenberg methods were employed for single-crystal investigations. All manipulations of the anhydrous bromides were performed in a nitrogen-filled glovebox which was purged of both oxygen and water. During transfer between the glovebox and the reaction system, samples were transported in evacuated containers or under atmospheres of dry nitrogen. Powder x-ray samples were coated with paraffin oil to retard further reaction with moisture during transfer and exposure. Diffraction data for the hydration products were obtained by exposure of anhydrous bromide samples which had not been coated with oil. Weissenberg samples were selected under oil and sealed in glass capillaries. Elemental analyses of products were effected for samarium by direct ignition (950°C) to the oxide and for bromide by a gravimetric silver halide procedure. The results were corrected for oxygen contamination which occurred as highly crystalline SmOBr. The oxide bromide was determined gravimetrically by dissolution of the bromide in water, adjustment of the pH to 4 with dilute nitric acid, and collection of the insoluble residue by filtration.

Results

Samarium Tribromide. The products obtained from the matrix dehydration procedures are cream-colored polycrystalline solids which react rapidly with moisture to form a white hydrate. Powder x-ray data for the products show only lines assignable to the orthorhombic $PuBr_3$-type tribromide (a = 4.042 (2), b = 12.706 (9), c = 9.124 (7) Å). The lattice parameters are in good agreement with the single-crystal data

of Zacharaisen.[7] Analytical data for a representative sample of the tribromide are presented in Table I. Diffraction data for the hydration product are indexable on a monoclinic $NdCl_3 \cdot 6H_2O$-type structure (a = 10.03 (1), b = 6.762 (5), c = 8.158 (8) Å; β = 93.57 (9)°).

Samarium Dibromide. The products obtained by reduction of the tribromide under hydrogen flow are fused polycrystalline black solids which exhibit a dark green color in the finely divided state. On exposure to air, the material forms a deep red solid which turns white on extended exposure to moisture. The results of chemical analysis in Table I and the x-ray powder data are consistent with the dibromide composition. The powder patterns are assignable to a tetragonal $SrBr_2$-type structure (a = 11.588 (4), c = 7.100 (3) Å); data for the red products are indexable on orthorhombic symmetry (a = 9.178 (4), b = 11.427 (7), c = 4.315 (2) Å) and show systematic extinctions consistent with space group *Pnma*. These results indicate that the red product is a $BaCl_2 \cdot H_2O$-type dibromide monohydrate. X-ray data show that the white hydration product is the tribromide hexahydrate. The dibromide forms deep red aqueous solutions which decolorize slowly on exposure to air and rapidly with effervescence upon the addition of acid.

Careful examination of the x-ray data for the dibromide showed the presence of a weak reflection (d = 2.794 Å) which was unassignable to the $SrBr_2$-type structure, and microscopic examination of the acidified (pH 4) aqueous solutions of the dibromide showed the presence of insoluble clear platelets. Isolation and x-ray analysis of the crystals showed that they were SmOBr. The refined lattice parameters obtained for the tetragonal PbFCl-type oxide bromide are a = 3.949 (2) and c = 7.913 (4) Å. Analytical results show that the levels of oxide bromide contamination of the dibromide products were all less than 0.5 mass %, a value which establishes the upper limit for oxygen contamination of the initial tribromide samples.

Powder diffraction data for products prepared by reaction of the metal with the tribromide showed the presence of the dibromide but frequently contained additional reflections which are unassignable either to $SrBr_2$-type $SmBr_2$ or to SmOBr. The presence and position of the extra lines are independent of container material, and the possibility that the unknown phase(s) resulted from reaction with the container was excluded. Further investigation showed that extended heating results in the disappearance of the extra lines and that they are indexable on an orthorhombic $PbCl_2$-type system (a = 7.973 (2), b = 4.753 (2), c = 9.503 (3) Å). These preliminary results suggested that the dibromide is dimorphic.

Subsequent investigation showed the existence of two bromide phases near x = 2. The products obtained by quenching hydrogen-reduced $SmBr_2$, from various temperatures, are all the black $SrBr_2$-type phase. The products from fusion of the dibromide with metal are deep brown-red, and their powder diffraction data indicate that all metal-rich compositions ($1.75 < x < 1.95$) contained only the $PbCl_2$-type dibromide. Evidence for the existence of lower bromides is not observed, and lattice parameters for the $PbCl_2$-type phase are independent of x. Although metallic samarium could not be detected by x-ray methods, its presence is indicated by the results of chemical analysis and optical microscopy. A final Br:Sm ratio of 1.91 was found for a product from an initial composition of x = 1.85. Microscopic examination of this sample showed the presence of small particles which exhibited a metallic luster and tarnished rapidly on exposure to air. The finely divided metal presumably reacts with atmospheric oxygen and water to form amorphous oxide and hydrated oxide. The metal is present in low concentrations, and failure to observe its diffraction pattern may result from the introduction of mechanical strain during sample preparation. Attempts to anneal crushed samples resulted in the loss of metal vapor, which was accompanied first by the coexistence of $PbCl_2$- and $SrBr_2$-type phases and resulted ultimately in complete conversion of the sample to the $SrBr_2$-type product. Loss of metal by reaction with the graphite container was not evident, but this possibility cannot be excluded since the lanthanide dicarbides are also metallic air-sensitive materials. Lattice parameters for the coexisting bromide phases are in excellent agreement with those for the respective modifications in the two-phase regions bracketing the x = 2 composition. An attempt to prepare $PbCl_2$-type $EuBr_2$ by analogous procedures was unsuccessful.

Intermediate Samarium Bromides. Fused black products are also obtained by reduction of the tribromide under static hydrogen atmospheres; however, the mass losses observed for the shorter reaction times are less than the theoretical values by up to 20%. Chemical analysis of one such product shows a Br:Sm ratio of 2.15. The powder x-ray diffraction patterns contain numerous broad reflections which are unassignable to either the dibromide or the tribromide. These products are also very reactive to moisture and form red aqueous solutions like those of the dibromide.

Characterization of the products from reaction of selected $SmBr_2$–$SmBr_3$ mixtures ($2.05 < x < 2.50$) in gold confirm the existence of an intermediate composition. For $x \leq 2.10$, the $SrBr_2$-type dibromide is found to coexist with the intermediate phase; for $x > 2.18$, the intermediate phase is observed to coexist with the $PuBr_3$-type tribromide. In the intermediate range, $2.10 < x < 2.18$, the products which were rapidly cooled or quenched from 800° give diffuse diffraction patterns like those observed for the products of hydrogen reduction. Diffraction data for several annealed products in the intermediate range show the presence of three different diffraction patterns.

Data for the larger samples prepared in graphite confirm the existence of three intermediate phases. Analytical data for products which were prepared to give crystallographically pure samples of the three phases appear in Table I; the x-ray diffraction patterns for these samples are presented in Table II. The Br:Sm ratios of these products ($SmBr_{2.129}$, $SmBr_{2.140}$, and $SmBr_{2.172}$) correspond closely with the theoretical values for Sm_8Br_{17}, Sm_7Br_{15}, and Sm_6Br_{13}, respectively. Oxide bromide contamination of these samples was in the range of 1–2 mass %. The level of oxygen contamination was found to increase with the number of reaction cycles necessary for preparation of the sample and apparently resulted from hydration during manipulation and transfer. The preparation of analytical samples is complicated by the high degree of similarity in the diffraction patterns of the three phases and by the extremely unfavorable tie line relationship for the $SmBr_{2.172}$ + $SmBr_3$ two-phase region. The $SmBr_{2.129}$ phase is most readily indentified by an intense, well-resolved doublet at d = 4.304 and 4.243 Å, but the $SmBr_{2.140}$ and $SmBr_{2.172}$ patterns are very similar. The unique lines at d = 2.427 Å for $SmBr_{2.140}$ and at d = 3.101 Å for $SmBr_{2.172}$ and the existence of clearly resolved doublets in $SmBr_{2.172}$ are the primary distinguishing features.

Attempts to index the diffraction data for the intermediate phases on orthogonal and trigonal systems have been unsuccessful and efforts to obtain a single crystal of an intermediate phase have also failed. The presence of reflections which are systematically shifted, unshifted (e.g., d = 5.235, 2.573, 2.169 Å), or split as a function of composition suggest that the phases might be monoclinic. The Weissenberg data show that fused fragments which had been annealed at 450° are highly polycrystalline.

Observation of the preparative reactions under dynamic vacuum has provided information about the vaporization

Table II. X-Ray Diffraction Data for the Intermediate Samarium Bromide Phases[a,b]

$Sm_{2.129}$		$SmBr_{2.140}$		$SmBr_{2.172}$	
Rel[c] *I*	*d*, Å	Rel *I*	*d*, Å	Rel *I*	*d*, Å
w	7.092	w	7.067	w	7.028
w-m	5.236	w-m	5.234	w-m	5.235
m-s	4.304	m-s, b	4.275	m-s	4.285
m-s	4.243	w	3.830	m-s	4.269
w	3.821	w	3.714	w	3.837
w	3.705	w-m, b	3.366	w	3.722
m	3.368	w-m, b	3.225	w	3.371
w-m	3.233	w-m	3.071	w	3.357
w	3.179	w-m, b	3.025	w	3.225
w-m	3.083	w-m, b	2.966	w	3.214
vw	3.051	m, b	2.869	w-m	3.101
w	3.038	w-m	2.661	w-m	3.058
w-m	3.003	w-m	2.613	m, b	3.028
w-m	2.956	w-m	2.600	w-m	2.967
w	2.929	s	2.573	w-m	2.957
w	2.897	w	2.538	w-m	2.870
w	2.876	w	2.466	w	2.861
w-m	2.695	w-m	2.456	m-s	2.667
w-m	2.634	w	2.427	w-m	2.615
m	2.615	w-m	2.403	w	2.600
s	2.572	w-m	2.399	s	2.574
w-m, b	2.470	w-m	2.234	w	2.536
w	2.450	m	2.174	w-m	2.469
m	2.401	m	2.169	w-m	2.456
w	2.271	w	2.080	m	2.408
w	2,245	w	2.017	m	2.402
w-m	2.217			m	2.242
w	2.177			m	2.174
w-m	2.169			m	2.168
w	2.093			w-m	2.082
				w-m	2.020

[a] Only reflections with $d > 2.000$ Å are listed. [b] All samples were annealed at 450°C. [c] Key: s, strong; m, medium; w, weak; v, very; b, broad.

processes of the samarium bromides. Vapor transport of the dibromide suggests vaporization by a congruent process which presumably involves the monomeric gas. This reaction is well-known for the dihalides of europium.[6,8,9] Observed shifts in composition of the intermediate phases toward that of the dibromide indicate vaporization with the loss of tribromide or bromine. The deposition of dibromide in cooler zones and the formation of large quantities of mercury bromides in the nitrogen-cooled traps suggest the loss of tribromide as gaseous dibromide plus bromine. This observation suggests similarities between the intermediate samarium phases and europium tribromide which undergoes thermal decomposition to the dibromide plus bromine.[5,10]

Discussion

The general features of the samarium–bromine phase diagram at the 450°C section have emerged from the present investigation. The crystallographic and analytical data show five two-phased regions between Sm and $SmBr_3$. In addition to these terminal phases, two-phase regions are defined by $SmBr_2$, $SmBr_{2.129}$, $SmBr_{2.140}$, and $SmBr_{2.172}$. The equilibria at elevated temperatures are uncertain, and in particular the nature of the solid–liquid interface is unknown. The x-ray data in Table II strongly suggest that the intermediate phases have similar structures. Data for the quenched and rapidly cooled intermediate products show that the phases are highly disordered at high temperatures. In fact, the diffraction patterns of unannealed compositions in the range $2.12 < x < 2.18$ are indistinguishable.

Crystallographic data show that $SmBr_2$ ($SrBr_2$-type), $SmBr_3$, $SmBr_2 \cdot H_2O$, and $SmBr_3 \cdot 6H_2O$ are isostructural with the corresponding europium phases.[5] As expected, the lattice parameters for the anhydrous samarium bromides are consistently larger than the corresponding values for the europium bromides. Several lattice parameters for the hydrated phases are, however, inconsistent with the lanthanide contraction. The hydrated samples were obtained by reaction of the anhydrous bromide with atmospheric moisture, and attainment of the same levels of hydration would be difficult. The observed anomalies in these parameters apparently arise from small differences in water content. Likewise, the incorporation of trace quantities of water by the anhydrous bromides and the concomitant alteration of their lattice parameters has also been considered. The rigor of moisture exclusion in the Guinier procedures, the invariance of the diffraction data with the extent of hydration,[5] and the correspondence of europium bromide data collected by both Guinier and Debye–Scherrer methods[11] indicate that this effect is small.

An unequivocal definition of equilibria in the samarium–bromine system is difficult because of the similarities of the intermediate phases and because of the possible inclusion of extraneous components such as oxygen. The presence of oxide bromide in all of the reduced products demonstrates that the bromide phases characterized in this investigation are saturated with oxygen. The important considerations concern the levels of oxygen contamination and their effects on the stabilities of the bromides. Since the sums of metal and bromine contents in Table I are all equal to or greater than 99.9 (1) mass %, the levels of oxygen inclusion are certainly small. Insight may again be obtained by analogy to the europium system which has been characterized both by a phase investigation[5] and by equilibrium activity measurements.[6,7] The alteration of gaseous activities by addition of small quantities of metal oxide to the $EuBr_2(l) \rightarrow EuBr_2(g)$ and the $EuBr_3(s) \rightarrow EuBr_2(s) + {}^1/_2Br_2(g)$ systems is immeasurably small.[12] Similar intermediate phases are not observed in the europium–oxygen–bromine system,[11] and it is doubtful that the samarium phases are stabilized by oxygen; however, this possibility cannot be excluded.

Other potential sources of contamination are the variety of container materials which have been employed. No evidence has been observed for the incorporation of any container material in the products, but some containers are clearly more suitable than others. Evidence exists for an appreciable miscibility of the lanthanide elements in tantalum,[13] but this material and graphite, which reacts rather slowly with the lanthanide metals at the experimental temperature,[14] are most suitable for compositions with $x < 2$. Graphite, which has been successfully employed as an inert container for vaporization studies of liquid lanthanide dihalides,[5,8,9] appears to be uniquely suitable for both hydrogen reduction and for reaction of compositions with $x > 2$. Gold seems to be satisfactory for short reaction times. However, gold containers appeared to be slightly etched after extended (1 week) contact with the molten bromides, and their use was discontinued. The formation of free bromine by the intermediate phases precludes the use of tantalum for $x > 2$. The reaction of samples under an inert atmosphere might substantially reduce the magnitudes of composition changes from vaporization, but rigorous purification of the gases is difficult.

The occurrence of dimorphism for MX_2 phases is well documented,[15,16] and the existence of $SrBr_2$- and $PbCl_2$-type samarium bromides has been observed by other investigators.[17] The present results suggest that the relationship between the two samarium phases is unusual. The quenching experiments indicate that the products are not related by a normal thermal transition. At all experimental temperatures, only the $PbCl_2$-type phase coexists with Sm metal, and only the $SrBr_2$-type phase coexists with $SmBr_{2.129}$. These observations and the coexistence of the two products indicate a difference in their metal activities and require the existence of a sixth two-phase region between the $PbCl_2$- and $SrBr_2$-type phases.

Table III. Metal Halide Compositions Defined by the Homologous Series M_nX_{2n+1}

n	Theor X:M	Reported compositions	Ref
1	3.000	MX_3 phases	
3	2.333	$PrCl_{2.31}$, $NdCl_{2.33}$	23, 24
4	2.250	$NdCl_{2.25}$, $NdCl_{2.27}$, $YbCl_{2.26}$	24–26
5	2.200	$NdCl_{2.20}$, $SmCl_{2.20}$	24, 27
6	2.167	$SmBr_{2.172}$	This work
7	2.143	$SmBr_{2.140}$, $HoCl_{2.14}$	This work, 28
8	2.125	$SmBr_{2.129}$	This work
9	2.111	$DyCl_{2.11}$, $TmCl_{2.11}$	29, 30
10	2.100	$TmCl_{2.10}$	30
11	2.091	$TmCl_{2.090}$	30
12	2.080	$TmCl_{2.080}$	30
13	2.077	$TmCl_{2.074}$	30
15	2.067	$TmCl_{2.067}$	30
25	2.040	$TmCl_{2.040}$	30
∞	2.000	MX_2 phases	

Complete conversion of a sample to the $PbCl_2$-type material at the $x = 1.95$ composition indicates that the width of the two-phase region is less than 0.05 in x. Analytical data have not been obtained for the $PbCl_2$-type products because of the inability to quantify unbound samarium metal.

Apart from the phase diagram, the existence of the two structural types near $x = 2$ demonstrates that divalent samarium is readily accommodated by two markedly different structural arrangements, the seven- and eight-coordinate $SrBr_2$-type and the nine-coordinate $PbCl_2$-type structures. The radius ratio correlations of Baernighausen et al.[16] show that $SmBr_2$ is near the interface of stability for the two structure types. The possibility that one form is simply a nonstoichiometric derivative,[18] $SmBr_{2\pm x}$, of the other form is highly unlikely. The coexistence of the two phases and the invariance of their lattice parameters are inconsistent with this type of derivative relationship. Furthermore, the existence of a derivative relationship requires that the two structures be closely related.[18] The dissimilarity of the two structures is indicated by their subgroup–supergroup relationships,[19,20] which show that their space groups are subgroups of different highest symmetry supergroups. The $P4/n$ space group of $SrBr_2$ is a subgroup of the $Fm3m$ (CaF_2-type) supergroup, and the structure is derived from a cubic closest packed arrangement of metals. The *Pnma* space group of $PbCl_2$ is a subgroup of the $P6_3/mmc$ (anti-W_2C type) supergroup and the structure is derived from a hexagonal closest packed arrangement of metals.

The existence of unusual lanthanide dihalides and intermediate halide compositions is well-known, primarily from the reports of Corbett and coworkers, and they are described in comprehensive reviews by Brown[21] and Corbett.[22] A reexamination of the reported lanthanide chloride, bromide, and iodide intermediate phases[23–32] in Table III shows that their compositions are remarkably consistent with an M_nX_{2n+1} series. One or more representatives are known for $n = 3$–13 inclusive. Because of the increasing closeness of compositions with increasing n, assignment of the $n = 25$ member is obviously somewhat uncertain. Furthermore, the $MX_{2.40}$ ($LaI_{2.42}$,[31] $PrBr_{2.38}$,[32] $NdCl_{2.37}$[25]) and $MX_{2.29}$ ($NdCl_{2.786}$[24] and $YbCl_{2.30}$[16]) compositions cannot be readily assigned to the M_nX_{2n+1} series. Although there is disagreement about the compositions in the Nd–Cl system,[24,25] the $LaI_{2.42}$, $PrBr_{2.38}$, and $YbCl_{2.29}$ phases are clearly not members of the M_nX_{2n+1} series. They are, however, described by an M_nX_{2n+2} series as the $n = 5$ ($MX_{2.400}$) and $n = 7$ ($MX_{2.286}$) members. The $2n + 1$ series is an odd-integer subset of the $2n + 2$ series, but because of the limited occurrence of unique $2n + 2$ members, it seems to be the more suitable series. The M_nX_{2n+1} and M_nX_{2n+2} formulations are highly reminiscent of those for the so-called Magneli phases, e.g., M_nO_{3n-1} and M_nO_{3n-2}.[33]

It is interesting to examine the structural relationships of the samarium bromides and to speculate about possible structural origins of the intermediate phases. Both forms of the dibromide and the tribromide are of known structural types, and as the two-dimensional projections in Figure 1 demonstrate, the $PuBr_3$-type[7] tribromide and $PbCl_2$-type[16] dibromide are closely related structures. The $PuBr_3$-type structure (Figure 1a) is readily described by alternating layers of MX_2^+ and X^-.[34] Removal of the anion layers and generation of an MX_2 composition is possible for systems with either altervalent anions or altervalent cations. The relationship of the monoclinic YOOH-type structure[35] to $PuBr_3$ and UCl_3 types has been described previously[34] and is shown by the projection of hypothetical YOOH-type $SmBr_2$ in Figure 1b. In addition to the removal of anion layers, interconversion of the $PuBr_3$- and YOOH-type structures requires that alternate MX_2 layers be displaced by a half-unit along the projection axis and that all the layers be displaced slightly along [001] of the tribromide. It is interesting to note that the YOOH- and UCl_3-type structures are related directly by anion removal; i.e., the vertical displacement of alternate layers is not necessary. In either case, the resultant YOOH-type structure has seven-coordinate cations and is readily converted into the nine-coordinate $PbCl_2$-type structure (Figure 1c) by tilting the triangular-shaped MX_2 units from their parallel orientation with the layers and by slightly expanding the layers along [100] of the monoclinic structure. The positions of the distorted MX_2 layers are defined by the dashed lines in the right portion of Figure 1c. The displacive interconversion of these MX_2 structures is consistent with the existence of a zellengleich (same cell) subgroup–supergroup relationship of index 2, i.e., $z(2)$, between the *Pnma* space group of $PbCl_2$ and the $P2_1/m$ space group of YOOH.[19,20] Obviously an alternate terminology, crystallographic shear (CS),[33] might be employed to describe the relationship of the $PbCl_2$- and $PuBr_3$-type structures.

A particularly interesting feature of the $PuBr_3$- and $PbCl_2$-type bromides is that the trivalent and divalent metals assume almost identical nine-coordinate geometries in both structures. The coordination, which approaches eightfold in the $PuBr_3$-type phase,[36] is readily seen by consideration of the cation coordination polyhedra. In both structures the polyhedra are trigonal-prismatic columns normal to the projection axis. The ninefold coordination is achieved by occupancy of the rectangular prismatic faces with anions from three adjacent columns which are displaced relative to the column of interest by a half-unit translation along the projection axis.[34] In the $PbCl_2$-type structure, the columns form chains by corner sharing of anions with two adjacent columns at the same level along the projection axis. In the $PuBr_3$-type structure, all polyhedral columns are free-standing, i.e., do not share anions with adjacent columns.

The close similarity of the dibromide and tribromide structures and the apparent existence of the M_nX_{2n+1} homologous series suggest that the stabilities of intermediate samarium bromides may have structural origins. As is shown by the hypothetical structures in Figure 2, the homologous series compositions are obtained by regular retention of $PuBr_3$-type anion layers in a phase that is primarily $PbCl_2$-type dibromide. The coherent intergrowth of two $PbCl_2$-type regions with a single bromide layer is demonstrated by the structures in Figure 2a. The left portion of this projection shows the layering and clearly demonstrates that all metal atoms have essentially identical nine-coordinate geometries. If n MX_2 layers are found between successive anion layers, the incremental variation of n from 1 (MX_3) to ∞ (MX_2)

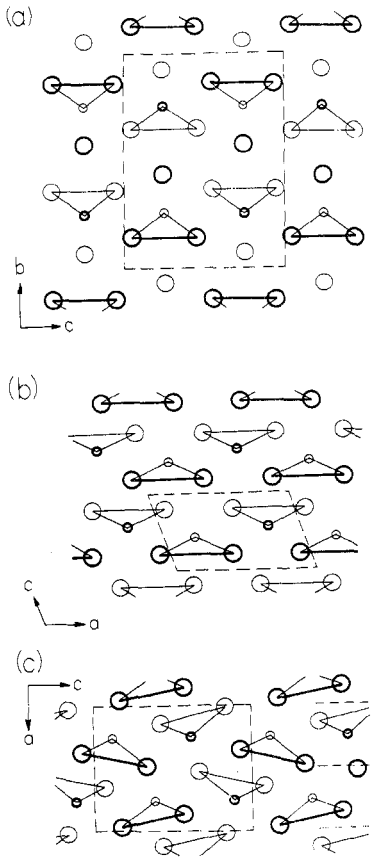

Figure 1. Structural relationships of the $PuBr_3$-type, YOOH-type, and $PbCl_2$-type structures. The projections are of (a) orthorhombic $PuBr_3$-type samarium tribromide on the (100) plane, (b) hypothetical YOOH-type samarium dibromide on the (010) plane, and (c) orthorhombic $PbCl_2$-type samarium dibromide on the (010) plane. (Large and small circles represent X and M, respectively. Light circles are at (a) $x = 1/2$, (b) $y = 1/4$, and (c) $y = 1/4$, and heavy circles are at (a) $x = 0$, (b) $y = 3/4$, and (c) $y = 3/4$. Positional coordinates are from ref 7, 16, and 35.)

generates all possible members of an M_nX_{2n+1} series. The right portion of Figure 2a shows the prismatic coordination polyhedra and demonstrates an alternate structural description. The intervening anion layers are seen to arise from regular discontinuities in the strings of corner-shared dibromide polyhedra. The similarity of x-ray diffraction data of the intermediate dibromides and the diffuse indistinguishable patterns observed for unannealed samples are consistent with an ordered layering sequence that is disordered at high temperatures. Figure 2b demonstrates the possibility of multiple anion layers (left) or multiple discontinuities in polyhedral sharing (right) and suggests the possibility for coherent intergrowth of slabs of $PbCl_2$-type dibromide with slabs of $PuBr_3$-type tribromide. The presence of $n - 1$ MX_2 layers between doubled anion layers like that in Figure 2b generates members of an M_nX_{2n+2} series.

The layered structures provide a reasonable explanation for the occurrence of the intermediate samarium bromides. Obviously, the intergrowth or crystallographic shear mechanism in Figure 2 is applicable only to halide systems which have $PbCl_2$-type dihalides and which presumably also have $PuBr_3$-type trihalides. The presence of any regular decrease in polyhedral sharing of in a dibromide structure, i.e., the intergrowth of dihalide and trihalide domains, would give rise to members of a homologous series. Hyde et al. have shown that the $PbCl_2$-type structure may be derived by crystallographic shear of the $UCl_3(Y(OH)_3)$-type structure and suggested that intermediate halide structures might be based on this relationship.[37] A similar model which also generates

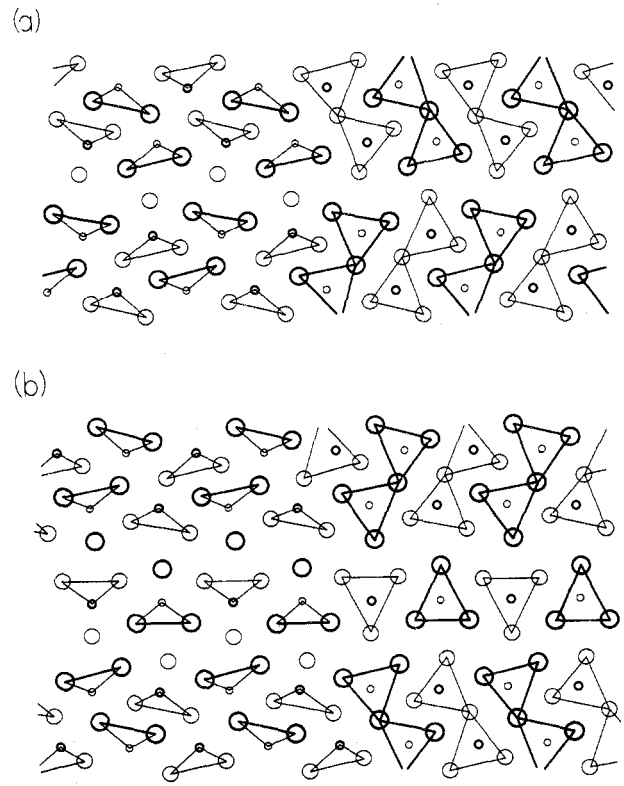

Figure 2. Projections of hypothetical intermediates samarium bromide structures. Part a shows the intergrowth of a single bromide layer in $PbCl_2$-type dibromide, and part b shows the intergrowth of a doubled anion layer in $PbCl_2$-type dibromide. (The identification key is the same as that for Figure 1c.)

an M_nX_{2n+1} series by layering of dihalide and trihalide has been proposed by Caro for the dysprosium and thulium chloride systems.[38] The apparent existence of homologous series and their possible derivation from parent MX_2 or MX_3 structures is clearly an emerging area of lanthanide halide chemistry.

The need for further work is obvious. Complex phase equilibria are to be expected for additional lanthanide halide systems, but the investigation of structural features of the intermediate phases seems most critical. If the structures are based on layering or a regular perturbation of parent structures, these systems might be amenable to lattice imaging techniques. The determination of intermediate structures would assist in the clarification of phase equilibria and contribute to the understanding of how structural properties and crystal chemical parameters affect the phase equilibria of solids.

Acknowledgment. Acknowledgment is made to the donors of the Petroleum Research Fund, administered by the American Chemical Society, for partial support of this research.

Registry No. $SmBr_2$, 50801-97-3; Sm_8Br_{17}, 57559-85-0; Sm_7Br_{15}, 57559-84-9; Sm_6Br_{13}, 57559-83-8; $SmBr_3$, 13759-87-0.

References and Notes

(1) W. Prandtl and H. Koegl, *Z. Anorg. Allg. Chem.*, **172**, 265 (1928).
(2) W. Klemm and J. Rockstroh, *Z. Anorg. Allg. Chem.*, **176**, 181 (1928).
(3) W. Doell and W. Klemm, *Z. Anorg. Allg. Chem.*, **241**, 239 (1939).
(4) J. G. Smeggil and H. A. Eick, *Inorg. Chem.*, **10**, 1458 (1971).
(5) J. M. Haschke and H. A. Eick, *J. Inorg. Nucl. Chem.*, **32**, 2153 (1970).
(6) J. M. Haschke and H. A. Eick, *J. Phys. Chem.*, **74**, 1806 (1970).
(7) W. H. Zachariasen, *Acta Crystallogr.*, **1**, 265, (1948).
(8) A. V. Hariharan and H. A. Eick, *High Temp. Sci.*, **4**, 91 (1972).
(9) A. V. Hariharan and H. A. Eick, *High Temp. Sci.*, **4**, 379 (1972).
(10) J. M. Haschke, *J. Chem. Thermodyn.*, **5**, 283 (1973).
(11) J. M. Haschke, Ph.D. Thesis, Michigan State University, East Lansing, Mich., 1969.
(12) J. M. Haschke, unpublished results.

(13) J. M. Haschke and H. A. Eick, *J. Am. Chem. Soc.*, **92**, 1526 (1970).
(14) J. M. Haschke, *Inorg. Chem.*, **14**, 779 (1975).
(15) K.-F. Seifert, *Fortschr. Mineral.*, **45**, 214 (1968).
(16) H. Baernighausen, H. P. Beck, and H.-W. Grueninger, *Proc. Rare Earth Res. Conf., 9th*, **1**, 74 (1971).
(17) H. Baernighausen, *Rev. Chim. Miner.*, **10**, 77 (1973).
(18) M. J. Buerger, *J. Chem. Phys.*, **15**, 1 (1947).
(19) J. Neubueser and H. Wondratschek, *Krist. Tech.*, **1**, 529 (1966).
(20) J. Neubueser and H. Wondratschek "Maximal Subgroups and Minimal Supergroups of the Space Groups", private communication with H. Wondratschek, University of Karlsruhe, Karlsruhe, West Germany, 1974.
(21) D. Brown, "Halides of the Lanthanides and Actinides", Wiley, New York, N.Y., 1968.
(22) J. D. Corbett, *Rev. Chim. Miner.*, **10**, 239 (1973).
(23) L. F. Druding, J. D. Corbett, and N. B. Ramsey, *Inorg. Chem.*, **2**, 869 (1963).
(24) G. I. Novikov and O. G. Polyachenok, *Zh. Neorg. Khim.*, **8**, 1053 (1963); *Russ. J. Inorg. Chem.*, **8**, 545 (1963).
(25) L. F. Druding and J. D. Corbett, *J. Am. Chem. Soc.*, **83**, 2462 (1961).
(26) N. A. Fishel and H. A. Eick, *J. Inorg. Nucl. Chem.*, **33**, 1201 (1971).
(27) O. G. Polyachenok and G. I. Novikov, *Zh. Neorg. Khim.*, **8**, 2818 (1963); *Russ. J. Inorg. Chem.*, **8**, 1478 (1963).
(28) U. Loechner and J. D. Corbett, *Inorg. Chem.*, **14**, 426 (1975).
(29) J. D. Corbett and B. C. McCollum, *Inorg. Chem.*, **5**, 938 (1966).
(30) P. E. Caro and J. D. Corbett, *J. Less-Common Met.*, **18**, 1 (1969).
(31) J. D. Corbett, L. F. Druding, W. J. Burkhard, and C. B. Lindahl, *Discuss. Faraday Soc.*, **32**, 79 (1961).
(32) R. A. Sallach and J. D. Corbett, *Inorg. Chem.*, **2**, 457 (1963).
(33) J. D. M. Bevan in "Comprehensive Inorganic Chemistry", Vol. 4, J. C. Bailar, Jr., H. J. Emeleus, R. Nyholm, and A. F. Trotman-Dickenson Ed., Pergamon Press, Oxford, 1973, Chapter 49.
(34) J. M. Haschke, *J. Solid State Chem.*, **14**, 238 (1975).
(35) A. N. Christensen, *Acta Chem. Scand.*, **19**, 1391 (1965).
(36) A. F. Wells, "Structural Inorganic Chemistry", 3rd ed, Oxford University Press, London, 1962, Chapter XXVI.
(37) B. G. Hyde, A. N. Bagshaw, S. Anderson, and M. O'Keeffe, *Annu. Rev. Mater. Sci.*, **4**, 43–92 (1974).
(38) P. E. Caro, *Natl. Bur. Stand. (U.S.), Spec. Publ.*, **No. 364**, 367 (1972).

Contribution from the Department of Chemistry, University of Canterbury, Christchurch, New Zealand

Crystal Structures of the Pentakis(trimethylarsine oxide)metal(II) Perchlorates [Ni(Me3AsO)5](ClO4)2 and [Mg(Me3AsO)5](ClO4)2

Y. S. NG, G. A. RODLEY,* and WARD T. ROBINSON

Received March 13, 1975 AIC50189H

The crystal structures of two isomorphous compounds, pentakis(trimethylarsine oxide)nickel(II) perchlorate, [Ni(Me3AsO)5](ClO4)2, and its magnesium analogue, have been determined by x-ray analyses. The compounds crystallize in the centrosymmetric space group $P2_1/n$, with four molecules in unit cells of dimensions a = 11.301 (3), 11.330 (5) Å, b = 27.256 (6), 27.562 (6) Å, c = 11.294 (5), 11.328 (6) Å, and β = 90.41 (3), 90.58 (5)° for the nickel and magnesium complexes, respectively. The structures were solved using diffractometer data and difference Patterson techniques. Least-squares refinements converged with final conventional R values of 0.064 (3975 data) and 0.068 (3552 data) for the nickel and magnesium complexes, respectively. The structures consist of discrete $[M(Me_3AsO)_5]^{2+}$ (M = Ni, Mg) cations well separated from perchlorate anions. The coordination geometry around the metal atoms is approximately square pyramidal, with nickel and magnesium atoms 0.359 (3) and 0.454 (3) Å above the least-squares plane of the basal oxygen and arsenic atoms, respectively. The arrangements of atoms around the central metal atoms are discussed in terms of the different electronic properties of magnesium and nickel. Small but significant differences between the two structures indicate the binding of the Me3AsO ligands is more than simple σ donation. Other structural features, notably a large cavity in the coordination sphere, also indicate that electronic rather than steric factors govern the structures of the cations.

Introduction

It is now apparent that monodentate oxo ligands of the type R_3XO (X = P, As) readily form five-coordinate complexes with metal(II) perchlorates.[1-7] Two basic types are obtained: $[M(R_3XO)_4ClO_4](ClO_4)^2$ and $[M(R_3XO)_5](ClO_4)_2$.[8] Preliminary x-ray photographic studies of $[Co(Ph_2MeAsO)_4ClO_4]ClO_4$ and $[Ni(Me_3AsO)_5](ClO_4)_2$ have shown the cations have essentially the same square-pyramidal structures.[2,8] We have now completed detailed analyses of the latter complex and its magnesium analogue using accurate diffractometer data sets.

The present results enable us to reassess the reasons for the formation of the square-pyramidal geometry in such systems. Previously attention was focused on steric factors. We now believe electronic binding properties of the oxo ligands are of prime importance. Also small but significant differences between the nickel and magnesium structures give further insight into the bonding of oxo ligands to metal ions.

Formation of five-coordinate complexes by non transition metal ions such as calcium and magnesium has not been studied extensively. However this geometry could be of considerable importance in biological systems.

While octahedral coordination may be the most common geometry for these ions, ligand systems with appropriate properties (electronic as well as steric) readily produce five-coordinate Ca^{2+} and Mg^{2+} complexes. The magnesium structure reported here provides detailed information on a magnesium complex, representative of a range of five-coordinate complexes of Ca^{2+} and Mg^{2+} recently prepared with oxo ligands.[9] A basically similar square-pyramidal structure has been found from an x-ray analysis of a chlorophyll-like aquomagnesium tetraphenylporphyrin.[10] Also a five-coordinate structure for certain chlorophyll systems has been indicated from infrared and NMR studies.[11] In other biological systems hydrophobic regions of protein structures may facilitate coordination numbers less than 6 through the elimination of water from the coordination sphere.

Experimental Section

Orange, plate-shaped crystals of $[Ni(Me_3AsO)_5](ClO_4)_2$ were grown from an acetonitrile solution in the presence of an ether vapor.[12] Colorless, transparent, plate-shaped crystals of $[Mg(Me_3AsO)_5](ClO_4)_2$ were provided by Mr. G. B. Jameson.[9] The nickel crystals, being sensitive to moisture, were sealed in capillary tubes under a stream of nitrogen. The crystals were assigned to the monoclinic system after examination by Weissenberg and precession photography, using Cu Kα radiation. Conditions limiting possible reflections were uniquely consistent with the monoclinic space group $P2_1/c$ but it was found convenient to solve both structures using the unconventional setting $P2_1/n$ (equivalent positions: x, y, z; $-x, -y, -z$; $1/2 + x, 1/2 - y, 1/2 + z$; $1/2 - x, 1/2 + y, 1/2 - z$). All data in this paper refer to this latter space group setting.

Unit cell parameters were obtained by least-squares analysis of the setting angles of 12 reflections accurately centered in a 5.0-mm